deterioration of concrete structures (Stewart 2011; Wang 2012). In the fifth assessment report (AR5) by the Intergovernmental Panel on Climate Change (IPCC), four representative concentration pathway (RCP) scenarios were introduced to describe possible climate futures and greenhouse gas (GHG) concentration trajectories in the years to come (Pachauri 2014). These factors influence carbonation processes and, thus, durability.

Corrosion of steel reinforcement is one of the main deterioration processes in RC structures that affect their serviceability and safety by reducing the strength, ductility and durability. Steel corrosion is generally initiated by chloride ingress or CO_2 interaction with alkali components of cement paste in the presence of water (Richardson 2003; Broomfield 2006; Bertolini 2013) and are expected to be affected by the climate change impacts (Wang 2012). Carbonation process can modify the concrete pore structure, alkalinity and binding capacity with a potential to yield steel corrosion and unsightly spalling as significant consequences.

Carbonation models in the literature can be classified into two main groups: comprehensive models based on a complete set of mass conservation equations (MCEs) for the participating reactants (Papadakis 1989; Papadakis 1991b; Cahyadi 1993; Burkan Isgor 2004; Khunthongkeaw 2005; Maekawa 2008; Park 2008; Kwon 2010; Talukdar 2012a) and simplified models that are generally expressed in the form of a square root of time for a determined carbonation depth (Papadakis 1991b; Papadakis 1991a; Yoon 2007; Vesikari 2009). The majority of the available studies on the progress of carbonation under projected climate change scenarios (e.g. Stewart 2011; Wang 2012; Bastidas-Arteaga 2013) are based on the simplified DuraCrete model (DuraCrete R17, 2000) and the consideration of SRES emission scenarios. Talukdar (2012) proposed a comprehensive carbonation model for climate change studies based on the governing MCEs of CO_2 and CH (Talukdar 2012a) and studied the climate change impacts on the progress of carbonation depth in Canadian RC structures (Talukdar 2012b). However, they did not consider the hygrothermal response of the internal concrete to environmental changes.

This paper summarises a comprehensive model and the consistent simplified model with time-dependent properties developed by the authors (Gharib 2016) for investigating the progress of concrete carbonation under projected climate change impacts. The validation of the proposed model and its application to climate change assessment is discussed, and an example presented.

2. CARBONATION MODEL

Carbonation processes significantly modify the pore structure of concrete, especially that of the paste. On one hand, carbonation reduces the porosity and pore size distribution of concrete, which improves the permeability and diffusivity properties but, on the other hand, it reduces the alkalinity of the pore solution by consuming the available alkali components and releasing some of the bound chlorides, both increasing the vulnerability of corrosion initiation. The carbonation process in concrete, and its major impacts on the concrete pore structure, are illustrated in Fig. 1. and discussed in the following section.

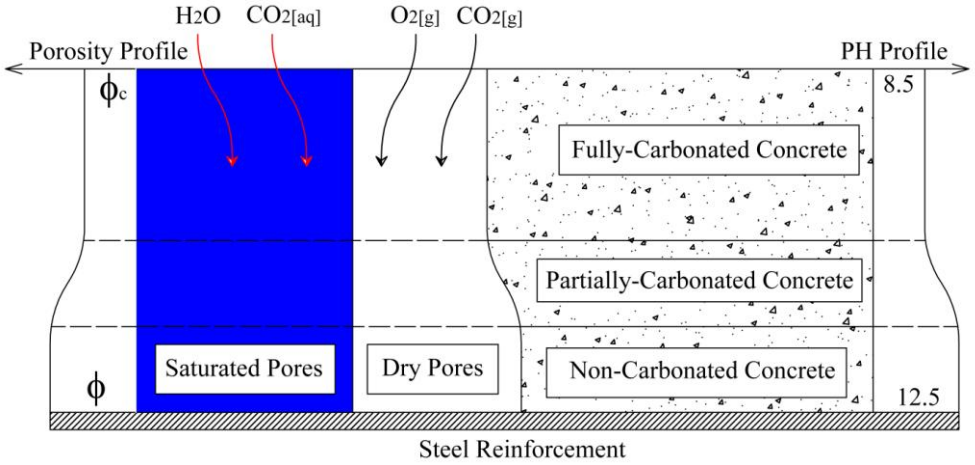

Fig. 1 Carbonation in concrete and its major impacts on the pore structure.

2.1 Comprehensive model

Referring to Fig. 1, atmospheric CO_2 diffuses from the surface into the concrete through unsaturated pores due to the difference in CO_2 concentration between the boundary air and the concrete; the reaction term for this transport is the dissolution rate of gaseous CO_2 in the pore solution. The dissolved CO_2 then moves through saturated pore volume via advection and diffusion mechanisms and reacts with the alkalis in the pore solution. By combining the governing transport equations of these two phases, the mass conservation equation (MCE) for the total concentration of CO_2 in concrete can be expressed as:

$$\frac{\partial}{\partial t}\left(\varepsilon[1-S][\mathrm{CO_2}]_{\mathrm{g}}+\varepsilon S[\mathrm{CO_2}]_{\mathrm{aq}}\right) - \nabla.\left(D_{\mathrm{c,g}}\nabla[\mathrm{CO_2}]_{\mathrm{g}}+D_{\mathrm{c,aq}}\nabla[\mathrm{CO_2}]_{\mathrm{aq}}-\mathbf{u}_w[\mathrm{CO_2}]_{\mathrm{aq}}\right)+Q_{\mathrm{c,c}}=0, \tag{1}$$

where ε and S are, respectively, the porosity and pore degree of saturation and $[CO_2]_g$ and $[CO_2]_{aq}$ are the molar concentrations of CO_2 in gas and dissolved phases, respectively. Furthermore, $D_{c,g}$ is the effective diffusivity of gaseous CO_2 in unsaturated pore volume and $D_{c,aq}$ is the effective diffusivity of dissolved CO_2 in the saturated pore volume, and $\mathbf{u}_w$ is the vector of advective (i.e. liquid water) velocities. These transport parameters are evaluated from the pore structure model and the hygrothermal model proposed by the authors (Gharib 2016). Lastly, $Q_{c,c}$ is the consumption rate of dissolved CO_2 in the carbonation reactions.

To reduce the number of independent variables, one may establish the following relationship between the concentrations of unreacted dissolved CO_2 and undissolved CO_2 at equilibrium state based on Henry's law and, assuming Arrhenius law for the temperature dependence of the associated rate constant:

$$[\mathrm{CO_2}]_{\mathrm{aq}}=H_{\mathrm{ref}}\exp\left[\frac{\Delta_{\mathrm{H}}}{R}\left(\frac{1}{T_{\mathrm{ref}}}-\frac{1}{T}\right)\right]RT[\mathrm{CO_2}]_{\mathrm{g}}, \tag{2}$$

where H_{ref} is Henry's constant for the dissolution of CO_2 at a reference temperature (H_{ref}=3.4×10^{-2} Lmol^{-1}atm^{-1} at T=298 K), and Δ_H is the enthalpy change or heat of CO_2 dissolution (Δ_H=20 kJmol^{-1}).

The other important reactant in the carbonation process is calcium hydroxide (CH), which is the major alkali component of cement paste. Solid CH dissolves in water and produces calcium (Ca^{2+}) and hydroxyl (OH^-) ions, where the dissolved calcium ions diffuse through the saturated pore volume and react with the dissolved CO_2 to form calcium carbonate that lines the pores. In addition, the consumption of hydroxyl ions in the carbonation reactions reduces the pH of the pore solution. The MCE for the molar concentration of total CH can be established similar to Eq. (1) as:

$$\frac{\partial}{\partial t}[\mathrm{CH}]_{\mathrm{total}} - \nabla.\left(D_{\mathrm{CH,aq}}\nabla[\mathrm{CH}]_{\mathrm{aq}} - \mathbf{u}_w[\mathrm{CH}]_{\mathrm{aq}}\right) + Q_{\mathrm{c,CH}} = 0, \tag{3}$$

where $[CH]_{aq}$ is the molar concentration of aqueous CH in the pore solution and $D_{CH,aq}$ is the effective diffusivity of aqueous CH, which is relatively small (of the order of 10^{-12} m^2/s). Moreover, $Q_{c,CH}$ is the molar consumption rate of CH in the carbonation reaction. There exists a maximum limit for the molar concentration of the dissolved CH at each time step that can be approximated by the solubility expression:

$$[\mathrm{CH}]_{\mathrm{aq,max}} = \sqrt[3]{\frac{1}{4}K_0 \exp\left(\frac{-\Delta_{\mathrm{CH}}}{RT}\right)}, \tag{4}$$

where the pre-exponential factor (K_0) and the heat of CH dissolution (Δ_{CH}) are, respectively, found to be 2.445×10^{-8} mol^{3}L^{-3} and -18.25 kJmol^{-1} to fit the experimental data (Maekawa 2008).

2.2 Simplified model

The comprehensive governing equation of CO_2 transport (see Section 2.1) can be simplified to a practical design equation by imposing two main assumptions: (a) neglecting transport of dissolved CO_2 and (b) seeking a solution for carbonation depth at steady-state conditions. Once the CO_2 flux into concrete is in balance with the rate of mass growth of bound CO_2, the following equilibrium statement can be made:

$$a_c x_c \mathrm{d}x_c = D_{\mathrm{g,c}}\Delta[\mathrm{CO_2}]_{\mathrm{g}}\,\mathrm{dt}, \tag{5}$$

where $\Delta[CO_2]_g$ is the difference in molar concentration of gaseous CO_2 between the environment and the non-carbonated concrete, and x_c represents the depth of fully carbonated concrete, below which full carbonation is achieved and beyond which CO_2 has not yet penetrated. Furthermore, a_c is the CO_2 binding capacity in fully carbonated concrete and represents the molar concentration of calcium oxide (CaO). The temporal dependencies of the diffusion coefficient and environmental concentration of CO_2 are taken as:

$$D_{\mathrm{g,c}} = D_{\mathrm{ref}}\left(t/t_{\mathrm{ref}}\right)^{-n_d} \quad \text{and} \quad \Delta[\mathrm{CO_2}]_{\mathrm{g}} = \Delta[\mathrm{CO_2}]_0\left(1+\mu_{\mathrm{gs}}t\right), \tag{6}$$

where D_{ref} is the diffusion coefficient at a reference time (t_{ref}) and $\Delta[CO_2]_0$ is the molar

concentration of atmospheric CO_2 at the start time of analysis. In addition, n_d is the aging exponent for CO_2 diffusivity, and μ_{gs} is the change rate for the surface concentration. The carbonation depth in concrete is then derived by integrating the LHS of Eq. (5) in space and the RHS in time, which can be expressed in the form of the well-known square root of time solution as:

$$x_c(t) = k_c\sqrt{t}, \tag{7}$$

where the time-dependent coefficient of carbonation (k_c) is obtained from:

$$k_c(t) = \sqrt{\frac{2D_{\text{ref}}\Delta[\text{CO}_2]_0}{a_c}\left(\frac{t}{t_{\text{ref}}}\right)^{-n_d}\frac{1}{1-n_d}\left(1+\frac{1-n_d}{2-n_d}\mu_{\text{gs}}t\right)}. \tag{8}$$

In the absence of temporal variations for the diffusivity of CO_2 and its boundary condition (i.e. n_d=0 and μ_{gs}=0), the coefficient of carbonation reduces to that proposed by Papadakis (1991).

3. MODEL VALIDATION AND NUMERICAL EXAMPLE

First, the accuracy of the presented carbonation model is verified with a selected set of experimental data in the literature. Then, the impacts of projected climate changes on the carbonation progress in concrete and the time to corrosion initiation are studied for an RC slab located in Sydney, Australia.

3.1 Validation example

The experimental test data of Talukdar (2012a) is used to show the accuracy of the presented model in capturing the carbonation progress under climate change impact. Talukdar (2012a) designed three climate change scenarios to evaluate the impact of change in environmental variables (temperature, relative humidity and CO_2 concentration) on the progress of carbonation; one of the scenarios, given in Table 1, is presented here as an illustrative example, with further examples given in (Gharib 2016).

Table 1 Experimental climate change scenarios of Talukdar (2012a)

Experimental Scenarios	T (°C)	H_R (%)	C_{CO2} (%)
Scenario A – Control	30	65	6
Scenario B – Variable temperature	25+(20/56)t	65	6

The experimental and numerical results of Talukdar (2012a) together with the model predictions of this study are presented in Figs. 2(a) and (b) for uncontaminated concrete under control scenario (scenario A) and variable temperature (scenario B), respectively. As can be seen, the predictions of the proposed model reasonably match the experimental data and capture the expected trend of change in carbonation progress. In addition, the numerical results show and improved accuracy compared to the simplistic model of Talukdar (2012a), which is mainly due to established coupling

with the microstructure-based hygrothermal model (Gharib 2016) that can improve the predictions of carbonation depth under variable environmental conditions.

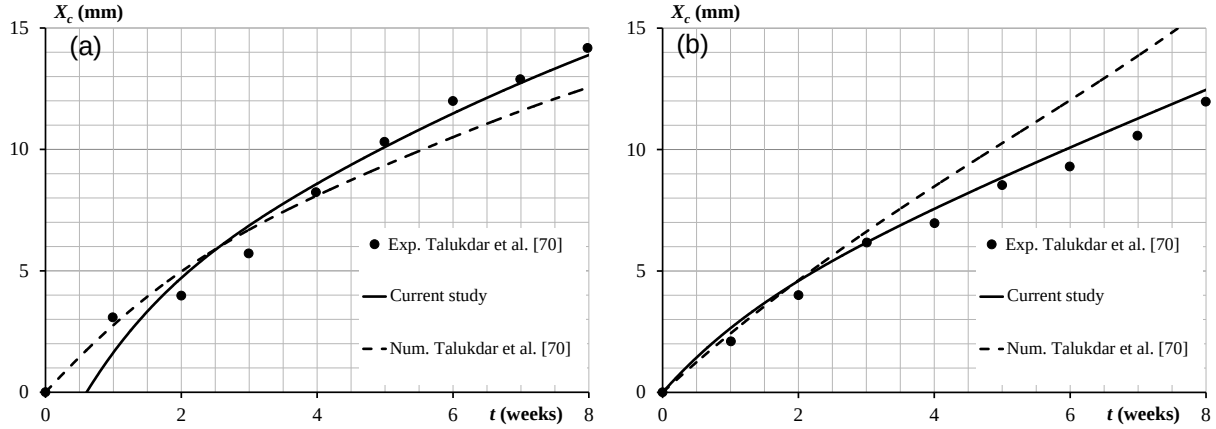

Fig. 2 Time-dependent development of carbonation depth in uncontaminated concrete under (a) control scenario, (b) variable temperature.

3.2 Climate change study

The propagation of carbonation depth in concrete, and the initiation period for subsequent corrosion, is studied for different environmental conditions. The impacts of the projected changes in the ambient temperature, relative humidity and atmospheric CO_2 content on the carbonation process are investigated through comparison of the simulation results under the projected climate change scenarios with those of the control scenario – the control scenario represents the case of no change in atmospheric CO_2. from 2015 values.

Three GHG concentration trajectories are considered for climate change projections and Sydney, Australia, with temperate climate conditions is selected as the location for this study. In order of severity, the trajectories are:

- RCP 2.6 (low), which assumes that global annual GHG emissions increase up to 2010-2020 and then decline substantially thereafter due to mitigations, and RF peaks at 3.0 W.m^{-2} and declines thereafter to stabilise at 2.6 W.m^{-2}.
- RCP 4.5 (medium-low) assumes that GHG emissions increase up to around 2040 and then decline, and RF stabilises at about 4.2 W.m^{-2} after 2100.
- RCP 8.5 (high) assumes that GHG emissions continue to increase throughout the 21st century without mitigation, and RF reaches 8.3 W.m^{-2} in 2100 on a rising trajectory.

The change in the environmental variables are modelled by:

$$V(t) = V_{avg} + \Delta V_0 \cos\left(\frac{\pi t'}{6}\right) + \Delta V_{\text{clim}}(t), \tag{9}$$

where V_{avg} and ΔV_0 are the annual average value and amplitude of the environmental variable (V), respectively, and ΔV_{clim} is the change in mean annual variable due to climate change. The seasonal variation of relative humidity generally has a time lag of about one month, compared to that of temperature (i.e. t' = t for temperature and t'≈ t – 0.08 year for relative humidity). The annual average and amplitude of each environmental variable are given Table 2 for Sydney (2105 values), and the projected change in the mean annual value at 2050 (ΔV_{2050}) and 2090 (ΔV_{2090}) with respect to the beginning of 21st century are listed for the different RCPs.

Table 2 Parameters for the change in the environmental variables for Sydney

Variable	V_{avg}	ΔV_0	RCP 2.6		RCP 4.5		RCP 8.5	
			ΔV_{2050}	ΔV_{2090}	ΔV_{2050}	ΔV_{2090}	ΔV_{2050}	ΔV_{2090}
T (°C)	17.5	5.5	1.0	1.0	1.3	1.8	1.7	3.7
H_R (%)	70.0	8.0	-0.8*	-1.4	-0.8	-1.7	-1.2	-1.8
C_{CO2} (ppm)	390	0.0	53	36	97	144	151	455

* Values for 2045 are substituted for smoothness and consistency.

For comparison of climate change impacts, time-dependent profiles of carbonation depth for an RC slab in Sydney, Australia, with different *w/c* ratios is shown in Fig. 3 for the considered RCPs. The dashed lines show projections of the carbonation depth if the trend for climate changes in the second 40 years were expected to be the same as that in the first 40 years. It is seen that the full line carbonation depth under RCP 8.5 is above the dashed line in the second 40 years, whereas this pattern reverses for RCP 2.6 and RCP 4.5 and the full line lies below the dashed line due to the considered mitigation influences in these scenarios.

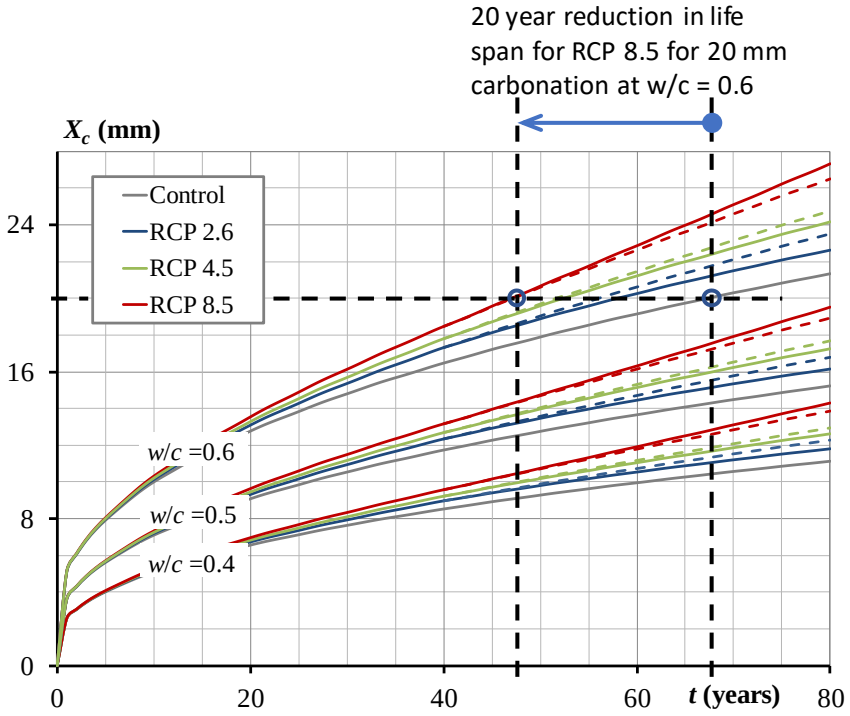

Fig. 3 Time-dependent carbonation depth of RC structures in Sydney for the considered *w/c* ratios and climate change scenarios.

Fig. 3 illustrates the impact of concrete quality and assumed climate change scenarios on the progress of carbonation and time to subsequent corrosion initiation in ideal conditions. As a qualitative example, the expected time to carbonation-induced corrosion initiation is about 67 years for an RC slab with a typical cover depth of 20 mm and *w/c* ratio of 0.6 under the control scenario without climate change. By increasing the severity of the introduced climate change, the initiation time reduces to about 58, 52 and 47 years under RCPs of 2.6, 4.5 and 8.5, respectively. In other words, the service life of this RC slab is expected to reduce by 14, 22 and 30 per cent under RCPs of 2.6, 4.5 and 8.5, respectively.

4. CONCLUSIONS

A multi-mechanistic carbonation model was presented to evaluate the progress of carbonation in concrete and initiation time to subsequent steel reinforcement corrosion. The proposed carbonation model was coupled with the microstructure-based hygrothermal model established by the authors. A consistent yet simplified model was also developed as the proposed revision for the commonly-used square root of time solution in international standards to facilitate carbonation studies under variable boundary conditions. The proposed model was validated against a selected set of semi-accelerated carbonation tests. The impacts of climate change projections on the initiation phase of carbonation-induced corrosion were numerically assessed for RC slabs in Sydney, which showed 30 per cent increase in carbonation depth under the pessimistic scenario (RCP 8.5). In conclusion, elevated greenhouse gas emissions

increase carbonation depth and show the highest impact among the influencing environmental parameters. Global warming increases the diffusivity of carbon dioxide and elevates the rate of carbonation reactions, both accelerating carbonation progress while reducing the solubility of carbon dioxide that partially cancels the imposed carbonation progress.

REFERENCES

Bastidas-Arteaga, E., Schoefs, F., Stewart, M.G. and Wang, X. (2013), "Influence of global warming on durability of corroding RC structures: A probabilistic approach", *Engineering Structures*. **51**, 259-266.

Bertolini, L., Elsener, B., Pedeferri, P., Redaelli, E. and Polder, R.B. (2013), *Corrosion of steel in concrete: prevention, diagnosis, repair*, John Wiley & Sons

Broomfield, J.P. (2006), *Corrosion of steel in concrete: understanding, investigation and repair*, CRC Press

Burkan Isgor, O. and Razaqpur, A.G. (2004), "Finite element modeling of coupled heat transfer, moisture transport and carbonation processes in concrete structures", *Cement and Concrete Composites*. **26**(1), 57-73.

Cahyadi, J. and Uomoto, T. (1993), "Influence of environmental relative humidity on carbonation of concrete (mathematical modeling)", *Durability of building materials and components*. **6**, 1142-1151.

DuraCrete R17 (2000), "General Guidelines for Durability Design and Redesign: Duracrete, Probabilistic Performance Based Durability Design of Concrete Structures", Document BE95-1347/R17, May 2000,. [Gouda]: [CUR].

Gharib, M. (2016), *Time-dependent numerical modelling of corrosion initiation in reinforced concrete structures under projected climate change impacts*, Phd Dissertation, The University of New South Wales.

Khunthongkeaw, J.T., S. (2005), "Model for Simulating Carbonation of Fly Ash Concrete", *Journal of Materials in Civil Engineering*. **17**(5), 570-578.

Kwon, S.-J. and Song, H.-W. (2010), "Analysis of carbonation behavior in concrete using neural network algorithm and carbonation modeling", *Cement and Concrete Research*. **40**(1), 119-127.

Maekawa, K., Ishida, T. and Kishi, T. (2008), *Multi-scale modeling of structural concrete*, CRC Press

Nakicenovic, N. and Swart, R. (2000), "Special report on emissions scenarios", *Special Report on Emissions Scenarios, Edited by Nebojsa Nakicenovic and Robert Swart, pp. 612. ISBN 0521804930. Cambridge, UK: Cambridge University Press, July 2000.*, **1**.

Pachauri, R.K., Allen, M., Barros, V., Broome, J., Cramer, W., Christ, R., Church, J., Clarke, L., Dahe, Q. and Dasgupta, P. (2014), "Climate Change 2014: Synthesis Report. Contribution of Working Groups I, II and III to the Fifth Assessment Report of the Intergovernmental Panel on Climate Change".

Papadakis, V.G., Vayenas, C.G. and Fardis, M.N. (1989), "A reaction engineering approach to the problem of concrete carbonation", *AIChE Journal*. **35**(10), 1639-1650.

Papadakis, V.G., Vayenas, C.G. and Fardis, M.N. (1991a), "Experimental investigation and mathematical modeling of the concrete carbonation problem", *Chemical Engineering Science*. **46**(5–6), 1333-1338.

Papadakis, V.G., Vayenas, C.G. and Fardis, M.N. (1991b), "Fundamental Modeling and Experimental Investigation of Concrete Carbonation", *Materials Journal*. **88**(4).

Park, D.C. (2008), "Carbonation of concrete in relation to CO2 permeability and degradation of coatings", *Construction and Building Materials*. **22**(11), 2260-2268.

Richardson, M.G. (2003), *Fundamentals of durable reinforced concrete*, CRC Press

Stewart, M.G., Wang, X. and Nguyen, M.N. (2011), "Climate change impact and risks of concrete infrastructure deterioration", *Engineering Structures*. **33**(4), 1326-1337.

Talukdar, S., Banthia, N. and Grace, J.R. (2012a), "Carbonation in concrete infrastructure in the context of global climate change – Part 1: Experimental results and model development", *Cement and Concrete Composites*. **34**(8), 924-930.

Talukdar, S., Banthia, N., Grace, J.R. and Cohen, S. (2012b), "Carbonation in concrete infrastructure in the context of global climate change: Part 2 – Canadian urban simulations", *Cement and Concrete Composites*. **34**(8), 931-935.

Vesikari, E. (2009), *Carbonation and chloride penetration in concrete with special objective of service life modelling by the Factor Approach. VTT Technical Research Centre of Finland*, VTT

Wang, X., Stewart, M. and Nguyen, M. (2012), "Impact of climate change on corrosion and damage to concrete infrastructure in Australia", *Climatic Change*. **110**(3-4), 941-957.

Yoon, I.-S., Çopuroğlu, O. and Park, K.-B. (2007), "Effect of global climatic change on carbonation progress of concrete", *Atmospheric Environment*. **41**(34), 7274-7285.